


Analytical asymptotics for hard diffraction

Anh Dung Le¹, Alfred H. Mueller,² and Stéphane Munier¹

¹*CPHT, CNRS, École polytechnique, IP Paris, Palaiseau F-91128, France*

²*Department of Physics, Columbia University, New York, New York 10027, USA*

 (Received 24 March 2021; accepted 19 July 2021; published 26 August 2021)

We show that the cross section for diffractive dissociation of a small onium off a large nucleus at total rapidity Y and requiring a minimum rapidity gap Y_{gap} can be identified, in a well-defined parametric limit, with a simple classical observable on the stochastic process representing the evolution of the state of the onium, as its rapidity increases, in the form of color dipole branchings: it formally coincides with twice the probability that an even number of these dipoles effectively participate in the scattering, when viewed in a frame in which the onium is evolved to the rapidity $Y - Y_{\text{gap}}$. Consequently, finding asymptotic solutions to the Kovchegov-Levin equation, which rules the Y dependence of the diffractive cross section, boils down to solving a probabilistic problem. Such a formulation authorizes the derivation of a parameter-free analytical expression for the gap distribution. Interestingly enough, events in which many dipoles interact simultaneously play an important role, since the distribution of the number k of dipoles participating in the interaction turns out to be proportional to $1/[k(k-1)]$.

DOI: [10.1103/PhysRevD.104.034026](https://doi.org/10.1103/PhysRevD.104.034026)

I. INTRODUCTION

Diffraction has been observed in the scattering of protons and nuclei [1,2]; more unexpectedly, also in deep-inelastic electron-proton scattering [3–5]. Diffractive events should represent a sizable fraction of the events seen at future electron-ion colliders [6,7], on the order of 20%–30% [8].

At high energies, electron-hadron scattering cross sections may always be calculated starting from onium-hadron cross sections. Indeed, in an appropriate frame, the electron-hadron interaction is mediated by a colorless quark-antiquark (onium) fluctuation of a virtual photon picked in the state of the electron [9,10] (see, e.g., Ref. [11] for an overview of high energy QCD).

Diffractive events are traditionally split into two classes: quasielastic scattering events, in which the diffractive system typically consists in a vector meson or in a hadronized open quark-antiquark pair, and high-mass diffractive dissociation events, in which the diffractive system possesses an invariant mass on the order of the center-of-mass energy of the onium-hadron subreaction, and a sizable multiplicity. While the former have drawn a lot of attention recently (see, e.g., Ref. [12] for a review), less effort has been devoted to the latter. In many works, the high-mass diffractive system is treated as a

quark-antiquark-gluon system (see, e.g., [8,13]), neglecting any further quantum evolution. While this is a fair approximation for phenomenological studies, the description of the parametric large-rapidity asymptotics requires us to account for all possible fluctuations.

An equation for the distribution of the rapidity gap in the form of an evolution in the total rapidity Y , here referred to as the Kovchegov-Levin (KL) equation, was established in Ref. [14], but only numerical solutions have been known [15]. Recently, based on a simple partonic picture of diffraction in which a gap of size Y_{gap} is due to an unusual fluctuation in the onium evolution at rapidity $Y - Y_{\text{gap}}$, the asymptotic functional form of that distribution was argued [16,17], in the limit of large rapidities and in the geometric scaling [18] kinematical region (see also Ref. [19] for an alternative calculation). But the overall numerical factor was believed not to be computable. In the present paper, we shall provide a parameter-free expression for the gap distribution, based on a new formulation of diffractive dissociation in terms of a probabilistic process.

Our starting point (Sec. II) will be the well-known relation between fixed impact-parameter semi-inclusive cross sections and S -matrix elements solutions of the Balitsky-Kovchegov (BK) equation [20,21]. In an appropriate limit, we shall derive a probabilistic formulation of diffraction, involving weights of the number of color-singlet effective independent exchanges between the diffractive system and the nucleus. Analytical expressions will be obtained for the latter (Sec. III), from which the diffractive cross section and the rapidity gap distribution will be derived (Sec. IV). We present our conclusions and

Published by the American Physical Society under the terms of the Creative Commons Attribution 4.0 International license. Further distribution of this work must maintain attribution to the author(s) and the published article's title, journal citation, and DOI. Funded by SCOAP³.

some prospects in Sec. V, and we report on a numerical check of our results in the Appendix.

II. FORMULATION OF SCATTERING CROSS SECTIONS

We consider the scattering of an onium of initial size r off a large nucleus. The relative rapidity of these colliding objects is denoted by Y . In the following, we shall rescale all the rapidity variables by multiplying them by $\bar{\alpha} \equiv \alpha_s N_c / \pi$. The kinematical rapidities will be written in capital letters, and the rescaled rapidities in lowercase letters; for example, we shall replace the total relative rapidity by $y \equiv \bar{\alpha} Y$.

Throughout this paper, we shall rely on the color dipole picture [22] to represent the Fock state of an onium of fixed initial size r by a random set of dipoles of various sizes $\{r_i\}$. It assumes the limit of infinite number N_c of colors, and is relevant in the large-rapidity limit. Technically, the dipole model can be seen as a tool to resum systematically all planar graphs that contribute to the probability of a given Fock state, keeping the terms that dominate when the onium is viewed in a frame in which it is very fast.

The distribution of these sets of dipoles depends on the rapidity of the onium in the reference frame in which it is probed. In the dipole picture, Fock states are elegantly generated by a simple $1 \rightarrow 2$ branching process in rapidity [22], which is a particular branching random walk (see, e.g., Ref. [23] for a review). The latter is defined by the rate of branching per unit rapidity $dp_{1 \rightarrow 2}(\underline{r}, \underline{r}')$ of a dipole of size vector \underline{r} into a pair of dipoles of size vectors $\{\underline{r}', \underline{r} - \underline{r}'\}$ (the common endpoint of these dipoles being localized within a surface of size $d^2 \underline{r}'$), which reads in QCD

$$dp_{1 \rightarrow 2}(\underline{r}, \underline{r}') \equiv \frac{d^2 \underline{r}'}{2\pi} \frac{r^2}{r'^2 |\underline{r} - \underline{r}'|^2}. \quad (1)$$

A. Matrix element for onium-nucleus forward elastic scattering

We shall express the onium-nucleus cross sections with the help of the forward elastic scattering matrix element S for a given set of dipoles present in the state of the onium at rapidity $\bar{y}_0 \equiv y - y_0$. At high energies, cross sections are purely absorptive, hence, in the conventions we shall use, the scattering amplitudes and the S -matrix elements are all real. Given that the dipoles are assumed to interact independently with the nucleus, we can write

$$S(y_0) = \prod_{\{r_i\}} S(y_0, r_i), \quad (2)$$

where $S(y_0, r_i)$ is the S -matrix element that encodes the scattering of a single dipole of size r_i off the nucleus (averaged over the fluctuations of the target nucleus), at

relative rapidity y_0 (which is the rapidity of the nucleus in the chosen frame.) This matrix element solves the BK evolution equation in rapidity y_0 [14], with as an initial condition at $y_0 = 0$ the onium-nucleus S -matrix element at zero relative rapidity taken, e.g., from the McLerran-Venugopalan model [24].

We recall that the BK equation is a nonlinear integro-differential equation which reads, for a function $\mathfrak{S}(y, r)$,

$$\partial_y \mathfrak{S}(y, r) = \int_{\underline{r}'} dp_{1 \rightarrow 2}(\underline{r}, \underline{r}') [\mathfrak{S}(y, r') \mathfrak{S}(y, |\underline{r} - \underline{r}'|) - \mathfrak{S}(y, r)]. \quad (3)$$

The initial condition is given in the form of a function of r only. We will refer to Eq. (3) as “BK $_{\mathfrak{S}}$.” The function $S(y_0, r_i)$ that appears in the right-hand side of Eq. (2) solves BK $_{\mathfrak{S}}$, with the identification $\mathfrak{S} \equiv S$. One may also write equivalently the BK equation for the function $\mathfrak{T} \equiv 1 - \mathfrak{S}$:

$$\partial_y \mathfrak{T}(y, r) = \int_{\underline{r}'} dp_{1 \rightarrow 2}(\underline{r}, \underline{r}') [\mathfrak{T}(y, r') + \mathfrak{T}(y, |\underline{r} - \underline{r}'|) - \mathfrak{T}(y, r) - \mathfrak{T}(y, r') \mathfrak{T}(y, |\underline{r} - \underline{r}'|)]. \quad (4)$$

Any equation in this form will be referred to as “BK $_{\mathfrak{T}}$.” Its solution is not known analytically. However, it has been established that for a wide class of initial conditions, which includes all the ones of interest for us, it tends asymptotically to a traveling wave [25]. Let us recall the main properties of this asymptotic solution.

We first need to introduce some background and a few useful notations. The integral kernel of the linearized equation (4) admits power functions of the form $\mathfrak{T}_\gamma(y, r) \equiv r^{2\gamma}$ as eigenfunctions. The eigenvalue equation reads

$$\int_{\underline{r}'} dp_{1 \rightarrow 2}(\underline{r}, \underline{r}') [\mathfrak{T}_\gamma(y, r') + \mathfrak{T}_\gamma(y, |\underline{r} - \underline{r}'|) - \mathfrak{T}_\gamma(y, r)] = \chi(\gamma) \mathfrak{T}_\gamma(y, r), \quad (5)$$

where $\chi(\gamma) \equiv 2\psi(1) - \psi(\gamma) - \psi(1 - \gamma)$, with the definition $\psi(\gamma) \equiv d \ln \Gamma(\gamma) / d\gamma$. Of particular importance for the physics we are investigating are the eigenvalues in the vicinity of the peculiar one $\chi(\gamma_0)$, where $\gamma_0 \in]0, 1[$ solves $\chi'(\gamma_0) = \chi(\gamma_0) / \gamma_0$ [26,27].

It will prove convenient to use, instead of the dipole size variable r , a logarithm of r . More precisely, we define

$$x \equiv \ln \frac{1}{r^2 Q_A^2}, \quad (6)$$

and call any such quantity a “log inverse size.” In this definition, Q_A is a fixed momentum scale characteristic of the nucleus. (It can be identified with the saturation momentum of the nucleus at rest, which emerges for example from the McLerran-Venugopalan model [24].)

The traveling wave that solves the $BK_{\mathfrak{Z}}$ equation at large rapidities is a smooth function connecting the fixed points 1 at $x \rightarrow -\infty$ and 0 at $x \rightarrow +\infty$. For a wide class of “steep-enough” initial conditions,¹ to which all the initial conditions we will need to consider belong, many properties of the traveling wave are independent of the latter. The transition between $\mathfrak{Z} = 1$ and $\mathfrak{Z} = 0$ is located around the value

$$X_y \equiv \chi'(\gamma_0)y - \frac{3}{2\gamma_0} \ln y \quad (7)$$

of x , within a region of typical size $1/\gamma_0$ (up to a nonuniversal y -independent term, and up to terms vanishing for large y). X_y is related to the rapidity-dependent saturation momentum $Q_s(y)$ through

$$X_y \equiv \ln \frac{Q_s^2(y)}{Q_A^2}. \quad (8)$$

The shape of \mathfrak{Z} ahead of this transition region reads

$$\mathfrak{Z}(y, x) \simeq \text{const} \times (x - X_y) e^{-\gamma_0(x - X_y)} \exp\left(-\frac{(x - X_y)^2}{2\chi''(\gamma_0)y}\right), \quad (9)$$

which holds in the limit of large y , and for values of x such that $1 \ll x - X_y \lesssim \sqrt{y}$.

Let us introduce the number density $n(x')$ of dipoles of log inverse size x' in a given realization of the onium Fock state evolved to the rapidity \tilde{y}_0 . In terms of n , $\mathcal{S}(y_0)$ in Eq. (2) becomes

$$\mathcal{S}(y_0) = \prod_{x'} [\mathcal{S}(y_0, x')]^{n(x') dx'}, \quad (10)$$

where the product now goes over all the bins in dipole log inverse size of infinitesimal width dx' . This also reads

$$\mathcal{S}(y_0) = \exp\left(-\int dx' n(x') \ln \frac{1}{\mathcal{S}(y_0, x')}\right) \equiv e^{-I(y_0)}, \quad (11)$$

with the definition

$$I(y_0) \equiv \int dx' n(x') \ln \frac{1}{\mathcal{S}(y_0, x')}. \quad (12)$$

Note that $I(y_0)$ is a random number, since n is a random distribution.

The S -matrix element for the scattering of the initial onium of log inverse size x at total relative rapidity y reads

$$S(y, x) = \langle \mathcal{S}(y_0) \rangle_{\tilde{y}_0, x}, \quad (13)$$

where the averaging is over all the dipole configurations of the onium at rapidity \tilde{y}_0 , namely over all realizations of n . The obtained function S is the same as the ones entering the expression of \mathcal{S} in Eq. (10), evaluated at a different rapidity.

B. Observables

Let us recall the relation between cross sections for onium-nucleus scattering at a fixed impact parameter \underline{b} per unit transverse surface $d^2\underline{b}$, and S -matrix elements.

(1) The total onium-nucleus cross section reads

$$\sigma_{\text{tot}}(y, x) = 2 \langle 1 - \mathcal{S}(y_0) \rangle_{\tilde{y}_0, x}. \quad (14)$$

(In this formula and in all the following ones, the \underline{b} dependence in \mathcal{S} and in the σ s is understood). The total cross section is obviously independent of the rapidity y_0 , although it is not manifest in the right-hand side of this equation.

(2) The diffractive cross section, with a rapidity gap not less than y_0 , coincides with the elastic cross section for the scattering of the Fock state of the onium at rapidity \tilde{y}_0 off the nucleus:

$$\sigma_{\text{diff}}(y, x; y_0) = \langle [1 - \mathcal{S}(y_0)]^2 \rangle_{\tilde{y}_0, x}. \quad (15)$$

This cross section is the sum of the purely elastic and of the diffractive dissociative cross sections.

(3) The inelastic cross section is the difference between the total cross section and the diffractive one. In terms of \mathcal{S} , it reads

$$\sigma_{\text{in}}(y, x; y_0) = \langle 1 - [\mathcal{S}(y_0)]^2 \rangle_{\tilde{y}_0, x}. \quad (16)$$

At variance with σ_{tot} , the diffractive and inelastic cross sections obviously depend on y_0 . Their rate of variation is related to the gap distribution, that we define as

$$\pi(y, r; y_{\text{gap}}) \equiv -\frac{1}{\sigma_{\text{tot}}} \frac{\partial \sigma_{\text{diff}}}{\partial y_0} \Big|_{y_0=y_{\text{gap}}} = \frac{1}{\sigma_{\text{tot}}} \frac{\partial \sigma_{\text{in}}}{\partial y_0} \Big|_{y_0=y_{\text{gap}}}. \quad (17)$$

So far, these expressions are fully accurate when so-called fan diagrams dominate the calculation of the S matrix. This is the case in the dipole model for QCD evolution of the onium Fock state, and when the scattering is off a very large nucleus.

C. Probabilistic picture

We now assume that in all the Fock state realizations which effectively contribute to cross sections, the scattering probability of each of the individual dipole is very small. In particular, the probability that the same dipole scatters more

¹ $\mathfrak{Z}(y = 0, x)$ has to decrease faster than $e^{-\gamma_0 x}$ when $x \rightarrow \infty$. Such solutions determined by the small- \mathfrak{Z} tail are called “pulled fronts” in the terminology of Ref. [28].

than once is negligible. Then $S(y_0, x')$ can be assumed to be close to 1 for all relevant values of x' in the expression of I defined in Eq. (12). For this reason, writing the latter in terms of $T = 1 - S$, we may keep the term linear in T , and drop higher powers of T . We denote by $I^{(1)}(y_0)$ the resulting overlap:

$$I^{(1)}(y_0) = \int dx' n(x') T(y_0, x'). \quad (18)$$

This integral corresponds to the sum of all possible diagrams in which one single dipole in one given realization of the onium Fock state, the content of which is fully encoded in the number density n , interacts by coupling to a single color-singlet gluon pair which mediates the interaction with the evolved nucleus. We shall call the approximation leading to Eq. (18) the “single-exchange approximation.”

We further define

$$F_N(\mathcal{I}) = \frac{\mathcal{I}^N}{N!} \quad \text{and} \quad G_k(\mathcal{I}) = F_k(\mathcal{I}) e^{-\mathcal{I}}. \quad (19)$$

$F_N[I^{(1)}(y_0)]$ is the quantum-mechanical amplitude corresponding to the sum of all the diagrams in which N dipoles present in the Fock state exchange color singlets with the nucleus at relative rapidity y_0 . $G_k[I^{(1)}(y_0)]$ is $F_k[I^{(1)}(y_0)]$ endowed with an extra $e^{-I^{(1)}(y_0)}$ factor that unitarizes it ($\sum_k G_k = 1$), turning it into a quantity that may be interpreted as a probability: it represents the probability that when choosing scattering configurations with a weight given by their amplitude $F_N[I^{(1)}(y_0)]$, one picks those in which exactly k dipoles interact. (Note that if the exponential is expanded, it is seen to resum an infinity of graphs). $G_k[I^{(1)}(y_0)]$ is also the probability that the set of dipoles that eventually interact with the nucleus, when the event is viewed from the restframe of the latter, are offspring of exactly k dipoles, at the rapidity y_0 relative to the nucleus. Both F_N and G_k are understood to be evaluated for a given Fock state realization of the onium.

We can now reformulate the scattering observables defined in Eqs. (14)–(16) in terms of these probabilities averaged over the realizations of the onium Fock state:

(i) The total cross section (14) simply reads

$$\begin{aligned} \sigma_{\text{tot}}(y, x) &= 2(1 - \langle G_0[I^{(1)}(y_0)] \rangle_{\tilde{y}_0, x}) \\ &= 2 \sum_{k=1}^{\infty} w_k(y, x; y_0), \end{aligned} \quad (20)$$

where the terms in the right-hand side are the average weights, defined as

$$w_k(y, x; y_0) \equiv \langle G_k[I^{(1)}(y_0)] \rangle_{\tilde{y}_0, x}. \quad (21)$$

Note that each weight w_k individually may *a priori* be frame dependent, i.e., depend upon y_0 , although the total cross section is boost invariant.

(ii) The inelastic cross section (16) can also be expressed in terms of w_k . We write

$$\sigma_{\text{in}}(y, x; y_0) = \langle (e^{I^{(1)}(y_0)} - e^{-I^{(1)}(y_0)}) e^{-I^{(1)}(y_0)} \rangle_{\tilde{y}_0, x} \quad (22)$$

and expand the difference of the exponentials to get

$$\sigma_{\text{in}}(y, x; y_0) = 2 \sum_{k \text{ odd}} w_k(y, x; y_0). \quad (23)$$

(iii) Likewise, the diffractive cross section (15) is then just twice the weight of the graphs in which an even number of dipoles interact:

$$\sigma_{\text{diff}}(y, x; y_0) = 2 \sum_{k \text{ even}} w_k(y, x; y_0), \quad (24)$$

where it is understood that the term $k = 0$ is excluded from this sum.

D. Comparison to the Kovchegov-Levin equation

We are going to show that the expression of the inelastic cross section in Eq. (23) in terms of the weights w_k is consistent with the solution to the KL equation.

1. Brief review of the Kovchegov-Levin equation

In this paragraph, we shall release the single-exchange approximation to review the exact equation for diffraction in the framework of the dipole model.

The KL equation, established in Ref. [14], can be expressed as an evolution equation (with the rapidity y) of the physical probability that there be no inelastic scattering between the state of the onium at \tilde{y}_0 and the nucleus,

$$S_{\text{in}}(y, r; y_0) \equiv 1 - \sigma_{\text{in}}(y, r; y_0) = \langle [S(y_0)]^2 \rangle_{\tilde{y}_0, r} \quad (25)$$

[see Eq. (16)]. The KL equation coincides with the BK $_{\mathfrak{S}}$ [Eq. (3)] equation, with the substitution $\mathfrak{S} = S_{\text{in}}$, and the initial condition

$$S_{\text{in}}(y_0, r; y_0) = [S(y_0, r)]^2. \quad (26)$$

Written in terms of the inelastic cross section σ_{in} and of the dipole amplitude T , this initial condition reads

$$\sigma_{\text{in}}(y_0, r; y_0) = 2T(y_0, r) - [T(y_0, r)]^2. \quad (27)$$

The rapidity gap distribution can easily be deduced from S_{in} , applying Eq. (17) to σ_{in} .

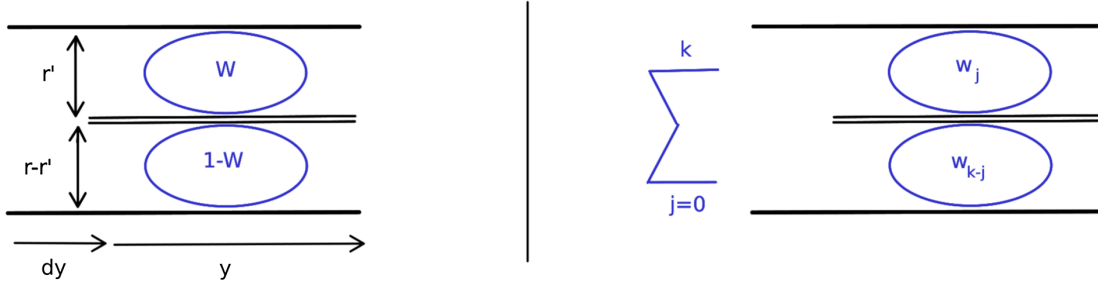


FIG. 1. Contributions of dipole splitting events to the evolution of W (left; this is one of the two possible configurations, the other one being deduced from the one displayed through the exchange $W \leftrightarrow 1 - W$), and of w_k (right).

2. Evolution of the inelastic cross section in the single-exchange approximation

We now turn to the inelastic cross section as given by Eq. (23), namely in the single-exchange approximation leading to Eq. (18) for the overlap.

Let us define $W(y, r; y_0)$ to be the weight of the graphs contributing to the onium-nucleus forward elastic scattering amplitude restricted to the diagrams in which there is an odd number of dipoles interacting with the nucleus boosted to the rapidity y_0 :

$$W(y, r; y_0) \equiv \sum_{k \text{ odd}} w_k(y, r; y_0). \quad (28)$$

The inelastic cross section (23) is just twice this quantity.

Using well-known techniques, we may easily establish an evolution equation for W with the total rapidity $y \geq y_0$. This goes as follows: we start from the rest frame of the onium, and increase the total rapidity of the scattering process by dy through a boost of the onium. In the small rapidity interval dy , the initial dipole of transverse size \underline{r} splits into a pair of dipoles of respective sizes $\{\underline{r}', \underline{r} - \underline{r}'\}$ with probability $dy dp_{1 \rightarrow 2}(\underline{r}, \underline{r}')$, or stays a single dipole with probability $1 - dy \int dp_{1 \rightarrow 2}(\underline{r}, \underline{r}')$. One notices that, if it splits, then the only contributions to $W(y + dy, r; y_0)$ come from the following configurations: the further fluctuations of one offspring eventually scatter an odd number of times, while the fluctuations of the other one either scatter an even number of times or do not scatter at all. The probability of such configurations reads

$$W(y, r'; y_0) \times [1 - W(y, |\underline{r} - \underline{r}'|; y_0)] + \{\underline{r}' \leftrightarrow \underline{r} - \underline{r}'\}. \quad (29)$$

The first term is illustrated in Fig. 1.

Putting together the contributions of all possible cases weighted by the corresponding probabilities, and letting $dy \rightarrow 0$, we get the integro-differential equation

$$\begin{aligned} \partial_y W(y, r; y_0) = & \int_{\underline{r}'} dp_{1 \rightarrow 2}(\underline{r}, \underline{r}') [W(y, r'; y_0) \\ & + W(y, |\underline{r} - \underline{r}'|; y_0) \\ & - 2W(y, r'; y_0)W(y, |\underline{r} - \underline{r}'|; y_0) \\ & - W(y, r; y_0)]. \end{aligned} \quad (30)$$

The three first terms under the integral in the right-hand side come from the splitting events, the last term from nonsplitting events. For $y = y_0$, the rapidity at which we want to take the initial condition, the onium Fock state reduces to a single dipole of size r : W then just equals the amplitude T at $y = y_0$,

$$W(y_0, r; y_0) = T(y_0, r). \quad (31)$$

Comparing Eq. (30) with Eq. (4), we see that the function $2W$ obeys $\text{BK}_{\mathfrak{Z}}$, but with as an initial condition² $W(y_0, r; y_0) = 2T(y_0, r)$, namely the first term of the initial condition Eq. (27) for the KL equation. We note that this term is dominant in the parametric region in which $T \ll 1$, and this allows us to argue that the solutions of the KL equation on the one hand, and $2W$ on the other hand, match asymptotically. Indeed, this stems from a general property of nonlinear equations in the class of the Fisher [29] and Kolmogorov-Petrovsky-Piscounov [30] equation, to which the $\text{BK}_{\mathfrak{Z}}$ equation belongs [25]. The large-rapidity solutions of such equations are essentially determined by the shape of the small- r (i.e., large positive- x) tail of the initial condition [28]. In this region, $2T - T^2 \simeq 2T$: the two functions taken as initial conditions coincide, and thus, the large- y solutions are the same. Therefore, for our purpose of deriving the exact asymptotics of solutions to the KL equation, we can safely trade σ_{in} for twice the sum W of all odd weights, and consequently, σ_{diff} for twice the sum of all even weights, as in Eq. (24).

²As a side remark, $2T$ is a function that takes values between 0 and 2, while the stable fixed point of Eq. (4) is $\mathfrak{Z} = 1$, which is a bit unusual.

III. ANALYTICAL ASYMPTOTICS FOR THE WEIGHTS OF THE NUMBER OF PARTICIPATING DIPOLES

A. Heuristic calculation

In this section, we shall compute the w_k s from their definition (21) as the probability that exactly k dipoles in the Fock state of the onium at rapidity \tilde{y}_0 interact with the nucleus boosted to the rapidity y_0 . The main ingredient is the overlap integral $I^{(1)}$ defined in Eq. (18). T in there is the forward elastic scattering amplitude of a dipole, which solves the Balitsky-Kovchegov equation, with as an initial condition, the scattering amplitude of a dipole off a nucleus at zero rapidity: its expression is derived from Eq. (9).

We will also need the form of the dipole number density n in realizations of the QCD evolution, endowed with its distribution, in order to be able to take the expectation value in Eq. (21). It is not known analytically: therefore, we shall use the phenomenological model for QCD evolution to represent the dipole content of the onium. This model was introduced in Ref. [31] for general branching random walks, and recently used in the context of QCD in Ref. [32]. We start with a brief review of the phenomenological model, before giving the expression of the overlap integral. We will then be in a position to calculate the weights w_k .

1. Formulation of the phenomenological model

The main assumption of the phenomenological model is that the onium Fock state evolves deterministically, except for one single fluctuation consisting in one unusually large dipole produced at some random rapidity \tilde{y}_1 , which, subsequently to its emission, also evolves deterministically until the scattering rapidity \tilde{y}_0 .

The deterministic, or “mean-field,” evolution of dipoles can be taken from the study of Ref. [31].³ Its calculation relies on the observation that the dipole density in a given realization of the high-energy evolution of an onium looks typically like the solution to the Balitsky-Fadin-Kuraev-Lipatov equation [33–35] in dipole form [22], when this equation is supplemented by a cutoff on the large-dipole-size tail. The latter is placed in such a way that at each step of the evolution, the dipole density as a function of the dipole log-size goes to zero for log-sizes larger than some predefined number of order unity from the log-size for which the latter density is equal to one. Physically, such a cutoff takes account of the fact that the dipole density in a given realization is actually a discrete distribution which has a largest dipole, a property which is not captured by the

³Actually, Ref. [31] addressed more general one-dimensional branching random walks, a class to which the dipole model belongs when restricted to a fixed impact parameter, or when focusing on the evolution towards larger dipole-sizes, as in the present context.

plain Balitsky-Fadin-Kuraev-Lipatov equation since the latter evolves the mean dipole density.⁴

The calculation in Ref. [31] transposed to the dipole model shows that the mean-field dipole number density of log inverse size x' in an onium of initial log inverse size \mathfrak{X} , after evolution over the rapidity interval $\Delta\tilde{y}$, reads

$$\begin{aligned} \bar{n}(\Delta\tilde{y}, x' - \mathfrak{X}) &= C_1(x' - \mathfrak{X} - \tilde{X}_{\Delta\tilde{y}})e^{\gamma_0(x' - \mathfrak{X} - \tilde{X}_{\Delta\tilde{y}})} \\ &\times \exp\left(-\frac{(x' - \mathfrak{X} - \tilde{X}_{\Delta\tilde{y}})^2}{2\chi''(\gamma_0)\Delta\tilde{y}}\right) \\ &\times \Theta(x' - \mathfrak{X} - \tilde{X}_{\Delta\tilde{y}}), \end{aligned} \quad (32)$$

where $\tilde{X}_{\Delta\tilde{y}} = -\chi'(\gamma_0)\Delta\tilde{y} + \frac{3}{2\gamma_0}\ln\Delta\tilde{y}$. [There may be an additive constant of order unity, but in Eq. (32), it is either negligible compared to other terms, or, when exponentiated, absorbed into the overall constant.]

As for the distribution of the rapidity and size of the fluctuation, we introduce the joint probability density $p(\delta, \tilde{y}_1)$ that the log inverse size of the unusually large dipole be smaller by δ than the log inverse size of the typical largest dipole $\mathfrak{X} + \tilde{X}_{\tilde{y}_1}$, and that it occurs at rapidity \tilde{y}_1 . We assume that it coincides with the distribution of the relative log inverse size of the largest dipole at \tilde{y}_1 . The probability that there is at least one dipole with a size larger than some fixed size, from which one deduces $p(\delta, \tilde{y}_1)$ by simple derivation and change of variables, solves the equation $\text{BK}_{\mathfrak{X}}$, with as an initial condition an appropriate Heaviside distribution. Thus, for $\delta \gg 1$,

$$p(\delta, \tilde{y}_1) = C\delta e^{-\gamma_0\delta} \exp\left(-\frac{\delta^2}{2\chi''(\gamma_0)\tilde{y}_1}\right). \quad (33)$$

(Again, C is an undetermined numerical constant of order unity.)

The number density of dipoles of log inverse size x' at rapidity \tilde{y}_0 , starting with an onium of log inverse size x , reads

$$n(x') = \bar{n}(\tilde{y}_0, x' - x) + \bar{n}(\tilde{y}_0 - \tilde{y}_1, x' - x - \tilde{X}_{\tilde{y}_1} + \delta) \quad (34)$$

with probability $p(\delta, \tilde{y}_1)d\delta d\tilde{y}_1$. The first term in the right-hand side is the deterministic evolution of the initial dipole of log inverse size $\mathfrak{X} \equiv x$. The second term represents the particle density generated by the evolution of the fluctuation of initial log inverse size $\mathfrak{X} \equiv x + \tilde{X}_{\tilde{y}_1} - \delta$.

⁴The idea of modeling discreteness by imposing a moving absorptive boundary condition on a deterministic evolution equation for the mean density was first proposed in Ref. [36] in the general context of the study of stochastic fronts. It turns out that a similar cutoff was introduced independently in QCD in the context of the scattering of two dipoles [37], but in the latter work, it was not interpreted as a model for discreteness, but was argued to be necessary to preserve the unitarity of the amplitudes.

When $x - X_y$ is large, the former is necessarily small compared to the latter, and therefore, can be neglected.

2. Overlap

The overlap I of the particle number is given by Eq. (18), up to the replacement of n by the second term in Eq. (34), and of T by Eq. (9) with $\mathfrak{T} = T$. (We will call the overall numerical constant appearing in that formula C_2 .) Thus, in the phenomenological model, it reads

$$I_{\delta, \tilde{y}_1}^{(1)}(y, x; y_0) = \int dx' \bar{n}(\tilde{y}_0 - \tilde{y}_1, x' - x - \tilde{X}_{\tilde{y}_1} + \delta) T(y_0, x'). \quad (35)$$

Now we consider a fluctuation of size δ occurring at the rapidity $\tilde{y}_1 < \tilde{y}_0$ such that $\tilde{y}_0 - \tilde{y}_1 \gg 1$. We choose δ so that $x - X_y - \delta$ be positive, large compared to unity but small compared to $\sqrt{y_0}$, which is always possible if y_0 is large enough. This restriction is motivated by the fact that configurations in this class, which maximize the overlap integral $I^{(1)}$ multiplied by the probability of a fluctuation $p(\delta, \tilde{y}_1)$, turn out to be the dominant ones when computing the averages over the onium Fock states; see Ref. [32]. The calculation of $I^{(1)}$, rather straightforward in the regime of interest, was performed in the previous reference, and led to the following expression:

$$I_{\delta, \tilde{y}_1}^{(1)}(y, x; y_0) = C_1 C_2 \sqrt{\frac{\pi}{2}} [\chi''(\gamma_0)]^{3/2} e^{-\gamma_0(x - X_y)} \left(\frac{y}{y_1 \tilde{y}_1} \right)^{3/2} e^{\gamma_0 \delta}. \quad (36)$$

This formula is manifestly boost invariant, since it does not exhibit a dependence on y_0 . Therefore, in what follows, we shall cancel y_0 from the list of variables upon which $I^{(1)}$ depends.

3. Evaluation of the weights w_k

We are now ready to calculate the weights w_k . In the phenomenological model, this calculation is formulated as

$$w_k(y, x; y_0) \equiv \left\langle \frac{1}{k!} [I_{\delta, \tilde{y}_1}^{(1)}(y, x)]^k e^{-I_{\delta, \tilde{y}_1}^{(1)}(y, x)} \right\rangle_{\delta, \tilde{y}_1 \leq \tilde{y}_0} \quad (37)$$

where the average $\langle \cdot \rangle$ over the Fock states takes the form of an integration over the rapidity \tilde{y}_1 at which the fluctuation may occur, and over its size δ , weighted by their probability distribution $p(\delta, \tilde{y}_1)$. In other terms,

$$w_k(y, x; y_0) = \int_0^{\tilde{y}_0} d\tilde{y}_1 \int_0^{+\infty} d\delta p(\delta, \tilde{y}_1) \frac{1}{k!} [I_{\delta, \tilde{y}_1}^{(1)}(y, x)]^k e^{-I_{\delta, \tilde{y}_1}^{(1)}(y, x)}. \quad (38)$$

We start by computing the integral over δ only: this is just the density of the \tilde{y}_1 variable. After replacing p by its expression given in Eq. (33), using $I_{\delta, \tilde{y}_1}^{(1)}$ (denoted I) as an integration variable instead of δ , we write

$$\begin{aligned} \frac{\partial w_k}{\partial \tilde{y}_1}(y, x; y - \tilde{y}_1) &= \frac{C}{\gamma_0^2 k!} I_{0, \tilde{y}_1}^{(1)}(y, x) \int_{I_{0, \tilde{y}_1}^{(1)}(y, x)}^{\infty} dI \ln \frac{I}{I_{0, \tilde{y}_1}^{(1)}(y, x)} I^{k-2} e^{-I} \\ &\times \exp \left(-\frac{\ln^2 [I / I_{0, \tilde{y}_1}^{(1)}(y, x)]}{2\gamma_0^2 \chi''(\gamma_0) \tilde{y}_1} \right). \end{aligned} \quad (39)$$

Integrals of this form also appeared in Ref. [32]: it was argued that the last exponential can be replaced by 1, and the remaining integral could be performed in the relevant limit (see Appendix A in Ref. [32]). Here we improve the treatment of this integral: we write the last exponential in the form of a series,

$$\begin{aligned} \frac{\partial w_k}{\partial \tilde{y}_1}(y, x; y - \tilde{y}_1) &= \frac{C}{\gamma_0^2 k!} I_{0, \tilde{y}_1}^{(1)}(y, x) \sum_{n=0}^{\infty} \frac{1}{n!} \frac{(-1)^n}{[2\gamma_0^2 \chi''(\gamma_0) \tilde{y}_1]^n} \\ &\times \int_{I_{0, \tilde{y}_1}^{(1)}(y, x)}^{\infty} \frac{dI}{I} \ln^{2n+1} \left(\frac{I}{I_{0, \tilde{y}_1}^{(1)}(y, x)} \right) I^{k-1} e^{-I}. \end{aligned} \quad (40)$$

Note that for any $k \geq 2$, the integral is regular when $I_{0, \tilde{y}_1}^{(1)} \rightarrow 0$. But it is logarithmically divergent in the case $k = 1$, which will require a separate treatment.

We are now going to compute the leading terms in the joint large- \tilde{y}_1 , large- $|\ln I_{0, \tilde{y}_1}^{(1)}|$ (i.e., large $x - X_y$) limit. We will keep only the leading power of $I_{0, \tilde{y}_1}^{(1)}$, and resum the terms in the series which possess the maximum number of factors $|\ln I_{0, \tilde{y}_1}^{(1)}| \sim \gamma_0(x - X_y)$ for each power of $1/\sqrt{\tilde{y}_1}$. We shall first address the values of k larger than or equal to 2, which can all be treated in the same way, and then address the case $k = 1$.

Case $k \geq 2$.—It is useful to represent the logarithms that appear in Eq. (40) by derivatives of power functions. Then, the integral therein reads

$$\begin{aligned} \int_{I_{0, \tilde{y}_1}^{(1)}(y, x)}^{\infty} \frac{dI}{I} \ln^{2n+1} \left(\frac{I}{I_{0, \tilde{y}_1}^{(1)}(y, x)} \right) I^{k-1} e^{-I} &= \frac{\partial^{2n+1}}{\partial \alpha^{2n+1}} \Big|_{\alpha=0} \left\{ \left[I_{0, \tilde{y}_1}^{(1)}(y, x) \right]^{-\alpha} \times \Gamma \left[\alpha + k - 1, I_{0, \tilde{y}_1}^{(1)}(y, x) \right] \right\}, \end{aligned} \quad (41)$$

where Γ is the incomplete Euler-Gamma function

$$\Gamma(x, I) \equiv \int_I^\infty d\bar{I} \bar{I}^{x-1} e^{-\bar{I}}. \quad (42)$$

The leading log terms are obtained when all the derivatives with respect to α act on the factor $[I_{0,\tilde{y}_1}^{(1)}(y, x)]^{-\alpha}$, and the incomplete Gamma function is replaced by the complete one, which evaluates as the factorial $[(k-2)!]$. After trivial simplifications, we find

$$\frac{\partial w_k}{\partial \tilde{y}_1}(y, x; y - \tilde{y}_1) = \frac{C}{\gamma_0^2} \frac{1}{k(k-1)} I_{0,\tilde{y}_1}^{(1)} \ln \frac{1}{I_{0,\tilde{y}_1}^{(1)}} \sum_{n=0}^{\infty} \frac{(-1)^n}{n!} \frac{\ln^{2n} I_{0,\tilde{y}_1}^{(1)}}{[2\gamma_0^2 \chi''(\gamma_0) \tilde{y}_1]^n}, \quad (43)$$

where we have understood the variables upon which the function $I_{0,\tilde{y}_1}^{(1)}$ depends.

The leading-log series can easily be resummed in the form of an exponential. Replacing $I_{0,\tilde{y}_1}^{(1)}$ by its expression (36) and $(-\ln I_{0,\tilde{y}_1}^{(1)})$ by $\gamma_0(x - X_y)$, which amounts to neglecting constants and logarithms of y, y_1, \tilde{y}_1 compared to $x - X_y$, we get

$$\frac{\partial w_k}{\partial \tilde{y}_1}(y, x; y - \tilde{y}_1) = \frac{c}{\gamma_0} \frac{1}{\sqrt{2\pi\chi''(\gamma_0)}} \frac{1}{k(k-1)} (x - X_y) e^{-\gamma_0(x-X_y)} \left(\frac{y}{y_1 \tilde{y}_1}\right)^{3/2} \exp\left(-\frac{(x-X_y)^2}{2\chi''(\gamma_0)\tilde{y}_1}\right), \quad (44)$$

where we have defined the constant c as a product of the previously introduced undetermined numerical constants,

$$c \equiv CC_1 C_2 \pi [\chi''(\gamma_0)]^2. \quad (45)$$

The integration over the rapidity \tilde{y}_1 at which the fluctuation occurs,

$$w_k(y, x; y_0) = \int_0^{\tilde{y}_0} d\tilde{y}_1 \partial_{\tilde{y}_1} w_k(y, x; y - \tilde{y}_1), \quad (46)$$

is well defined, due to the last exponential in Eq. (44) which acts as a diffusive cutoff on small values of \tilde{y}_1 . We may write the integral with the help of an error function and of elementary functions as

$$\begin{aligned} \int_0^{\tilde{y}_0} d\tilde{y}_1 \left(\frac{y}{y_1 \tilde{y}_1}\right)^{3/2} \exp\left(-\frac{(x-X_y)^2}{2\chi''(\gamma_0)\tilde{y}_1}\right) &= \frac{\sqrt{2\pi\chi''(\gamma_0)}}{x-X_y} \left(1 - \frac{(x-X_y)^2}{\chi''(\gamma_0)y}\right) \operatorname{erfc}\left(\frac{x-X_y}{\sqrt{2\chi''(\gamma_0)}} \sqrt{\frac{y_0}{y\tilde{y}_0}}\right) \exp\left(-\frac{(x-X_y)^2}{2\chi''(\gamma_0)y}\right) \\ &+ 2\sqrt{\frac{\tilde{y}_0}{yy_0}} \exp\left(-\frac{(x-X_y)^2}{2\chi''(\gamma_0)\tilde{y}_0}\right). \end{aligned} \quad (47)$$

When $y \rightarrow \infty$, it boils down to two simple terms. Therefore, in this limit, w_k eventually reads

$$\begin{aligned} w_{k \geq 2}(y, x; y_0) &= \frac{c}{\gamma_0} \frac{1}{k(k-1)} \left(1 + \sqrt{\frac{2}{\pi\chi''(\gamma_0)}} \frac{x-X_y}{\sqrt{y_0}}\right) \\ &\times e^{-\gamma_0(x-X_y)}. \end{aligned} \quad (48)$$

Interestingly enough, the ratio $w_{k \geq 2}/w_2$ has a very simple expression:

$$\frac{w_{k \geq 2}}{w_2} = \frac{2}{k(k-1)}. \quad (49)$$

This shows that the distribution of the number of participating dipoles decreases only slowly at large k . The events

which involve many of them are not rare at all. As a matter of fact, the mean participant number is formally infinite.

Case $k = 1$.—In this case, it is convenient to change variable in the integral in Eq. (40). We define $l \equiv \ln[I/I_{0,\tilde{y}_1}^{(1)}(y, x)]$: the integral over I then becomes

$$\int_0^{+\infty} dl l^{2n+1} \exp\left(-I_{0,\tilde{y}_1}^{(1)}(y, x) e^l\right). \quad (50)$$

The exponential is tantamount to a cutoff effectively limiting the integration region to $[0, -\ln I_{0,\tilde{y}_1}^{(1)}(y, x)]$. For small $I_{0,\tilde{y}_1}^{(1)}$, we can replace it by a Heaviside-theta function, and hence perform trivially the integral. We get

$$\frac{1}{2n+2} \ln^{2n+2} I_{0,\tilde{y}_1}^{(1)}(y, x). \quad (51)$$

After resummation of the series of the leading logarithms of $I_{0,\tilde{y}_0}^{(1)}$ and simplifications along the same lines as those followed in the case $k \geq 2$, one finds

$$\frac{\partial w_1}{\partial \tilde{y}_1}(y, x; y - \tilde{y}_1) = c \sqrt{\frac{\chi''(\gamma_0)}{2\pi}} e^{-\gamma_0(x-X_y)} \frac{y^{3/2}}{y_1^{3/2} \sqrt{\tilde{y}_1}} \times \left[1 - \exp\left(-\frac{(x-X_y)^2}{2\chi''(\gamma_0)\tilde{y}_1}\right) \right]. \quad (52)$$

As in the case $k \geq 2$, we may integrate over the rapidity \tilde{y}_1 between 0 and \tilde{y}_0 . Now the singularity at $\tilde{y}_1 = 0$ is not cut off, but it is integrable. Since we assume that \tilde{y}_0 is on the order of y , and since we take x in the scaling region such that $(x-X_y)^2 \ll y$, the upper limit of the relevant integration region is on the order of $(x-X_y)^2$. We can approximate $(y/y_1)^{3/2}$ by 1, and set the upper bound to $+\infty$. The integral to perform takes the form

$$\int_0^\infty \frac{d\tilde{y}_1}{\sqrt{\tilde{y}_1}} \left[1 - \exp\left(-\frac{(x-X_y)^2}{2\chi''(\gamma_0)\tilde{y}_1}\right) \right] \simeq \sqrt{\frac{2\pi}{\chi''(\gamma_0)}} \times (x-X_y). \quad (53)$$

Hence, the weight of the contributions of a single participating dipole reads

$$w_1(y, x; y_0) = c(x-X_y) \times e^{-\gamma_0(x-X_y)}. \quad (54)$$

At this level of approximation, w_1 is manifestly boost invariant. Actually, what is rigorously boost invariant is the total cross section σ_{tot} , i.e., the series $2 \sum_{k \geq 1} w_k$. But the term $2w_1$ dominates this sum parametrically, since it has an extra $x-X_y$ factor with respect to all other terms.

B. Generating function

In this section, we will establish that a generating function of the weights w_k obeys a set of BK equations. We will conjecture the large-rapidity solution, and check it numerically.

1. Rapidity evolution of the weights and of their generating function

The set of weights $\{w_k, k \geq 0\}$ obeys a hierarchy of evolution equations,

$$\partial_y w_k(y, r; y_0) = \int_{\underline{r}'} dp_{1 \rightarrow 2}(\underline{r}, \underline{r}') \left(\sum_{j=0}^k w_j(y, r'; y_0) w_{k-j}(y, |\underline{r} - \underline{r}'|; y_0) - w_k(y, r; y_0) \right), \quad (55)$$

with the initial condition $w_k(y_0, r; y_0) = \delta_{k,0} S(y_0, r) + \delta_{k,1} T(y_0, r)$. The proof is straightforward, using well-known techniques; see Fig. 1 for a graphical illustration of the contribution of the nontrivial first term in the right-hand side.

The generating function

$$\tilde{w}_\lambda(y, r; y_0) = \sum_{k=0}^{\infty} \lambda^k w_k(y, r; y_0) \quad (56)$$

obeys a unique equation, which turns out to be the BK \mathfrak{S} equation (3), with $\mathfrak{S} \equiv \tilde{w}$. The initial condition at $y = y_0$ reads

$$\tilde{w}_\lambda(y_0, r; y_0) = 1 - (1-\lambda)T(y_0, r). \quad (57)$$

A few comments are in order. First, the unitarity of the probability that any scattering may occur reads, in terms of the generating function, $\tilde{w}_{\lambda=1}(y, r; y_0) = 1$. Second, the S -matrix coincides with the generating function evaluated at $\lambda = 0$: $\tilde{w}_{\lambda=0}(y, r; y_0) = S(y, r)$. Third, there is a direct

relation between the generating function evaluated at two different values of λ and the difference of the diffractive and inelastic cross sections:

$$2(\tilde{w}_{\lambda=-1} - \tilde{w}_{\lambda=0}) = \sigma_{\text{diff}} - \sigma_{\text{in}}. \quad (58)$$

2. Infinite-rapidity limit: traveling wave solution

In the infinite- y limit, the solution to the BK equation converges to a traveling wave also starting with the initial condition (57), namely that $\tilde{w}_\lambda(y, x; y_0)$ tends to a function of $x-X_y + f_{y_0}(\lambda)$ only, where X_y was given in Eq. (8), and f is a “delay function” that vanishes for $\lambda = 0$.

When furthermore $x-X_y + f_{y_0}(\lambda)$ is taken finite but large, the analytic form for the shape of the traveling wave front reads

$$1 - \tilde{w}_\lambda(y, x; y_0) = c[x-X_y + f_{y_0}(\lambda)] e^{-\gamma_0[x-X_y + f_{y_0}(\lambda)]}, \quad (59)$$

where c is an undetermined constant of order unity.

As for the delay function $f_{y_0}(\lambda)$, we may conjecture the formula

$$f_{y_0}(\lambda) = \frac{1}{\gamma_0} \ln \frac{1}{1-\lambda} \times \left(1 - \frac{1}{\gamma_0} \sqrt{\frac{2}{\pi \chi''(\gamma_0)} \frac{1}{\sqrt{y_0}}} \right). \quad (60)$$

This conjecture is motivated by the following observation. There exists a function $f_{y_0}(\lambda)$ such that the expression for $1 - \tilde{w}_\lambda(y_0, x; y_0)$ in Eq. (57), namely

$$c(1-\lambda)(x - X_{y_0}) e^{-\gamma_0(x - X_{y_0})} \quad (61)$$

can be matched to the regular (delayed) traveling wave (59) at $y = y_0$, in the region $\ln \frac{1}{1-\lambda} \ll x - X_{y_0} \ll \sqrt{y_0}$. Indeed, equalizing the two front shapes implies

$$e^{\gamma_0 f_{y_0}(\lambda)} = \frac{1}{1-\lambda} \times \left(1 + \frac{f_{y_0}(\lambda)}{\Delta} \right), \quad (62)$$

which can be solved iteratively as

$$f_{y_0}(\lambda) = \frac{1}{\gamma_0} \ln \frac{1}{1-\lambda} + \frac{1}{\gamma_0} \ln \left(1 + \frac{\frac{1}{\gamma_0} \ln \frac{1}{1-\lambda} + \frac{1}{\gamma_0} \ln \left(1 + \frac{f_{y_0}(\lambda)}{\Delta} \right)}{\Delta} \right). \quad (63)$$

For Δ satisfying the above ordering condition, the second logarithm may be expanded to first order, leading to a closed expression for the delay:

$$f_{y_0}(\lambda) \simeq \frac{1}{\gamma_0} \ln \frac{1}{1-\lambda} \left(1 + \frac{1}{\gamma_0 \Delta} \right). \quad (64)$$

Keeping λ fixed, choosing Δ of order say $y_0^{1/2-\epsilon}$ for some fixed $\epsilon \in]0, \frac{1}{2}[$ and letting y_0 become large, this expression clearly tends to the conjectured $f_\infty(\lambda)$, Eq. (60). Since the expression for $1 - \tilde{w}_\lambda(y_0, x; y_0)$ is that of a regular front which would have evolved from a step initial condition $\Theta(-x)$ in a large region from its tip, and since the large-rapidity position of a traveling wave is determined precisely by its shape in the tip region, we conclude that the solution for $1 - \tilde{w}_\lambda(y, x; y_0)$ indeed tends to a traveling wave at large y , with position X_y pulled back by the distance $f_{y_0}(\lambda)$. We expect this solution to be valid when $|\ln(1-\lambda)| \ll \sqrt{y_0}$, which is not a too restrictive condition,⁵ since we are eventually interested in the expansion of \tilde{w}_λ around $\lambda = 0$. We are not able to determine the finite- y_0 correction from these heuristics, but since Δ is at most $\sqrt{y_0}$, a subleading term of relative order $1/\sqrt{y_0}$ is plausible.

Note that $f_\infty(\lambda)$ is the known leading contribution to the delay when the initial condition for the BK_z equation (or for any equation in the same class) is a step function of height $1 - \lambda$ [38,39]. But in that case, $\frac{1}{\gamma_0} \ln \frac{1}{1-\lambda}$ represents the largest term in the expression of the delay in the limit $\lambda \rightarrow 1$, and there is a subleading nonanalytic term $-\frac{1}{\gamma_0} \ln[-\ln(1-\lambda)]$.

The numerical coefficient of the subleading term is chosen in order to recover the expressions for w_k found above in the phenomenological model. Indeed, the shape of the traveling wave (59) with $f_{y_0}(\lambda)$ being replaced by Eq. (60) can be expanded in the power series (56) of λ , leading to expressions for the w_k s. Let us outline the main steps of the calculation.

Starting from Eq. (59), replacing f in there by Eq. (60), we get

$$1 - \tilde{w}_\lambda(y, x; y_0) = c(1-\lambda)^{1-\frac{1}{\gamma_0} \sqrt{\frac{2}{\pi \chi''(\gamma_0)} \frac{1}{\sqrt{y_0}}}} \left[x - X_y + \frac{1}{\gamma_0} \ln \frac{1}{1-\lambda} \left(1 - \frac{1}{\gamma_0} \sqrt{\frac{2}{\pi \chi''(\gamma_0)} \frac{1}{\sqrt{y_0}}} \right) \right] e^{-\gamma_0(x - X_y)}. \quad (65)$$

Next, we expand for large y_0 , dropping all higher powers of $1/\sqrt{y_0}$, and the terms of order $1/\sqrt{y_0}$, which are not enhanced by a power of $x - X_y$. The generating function then reads

$$1 - \tilde{w}_\lambda(y, x; y_0) = \left[c(1-\lambda)(x - X_y) + \frac{c}{\gamma_0} (1-\lambda) \ln \frac{1}{1-\lambda} \left(1 + \sqrt{\frac{2}{\pi \chi''(\gamma_0)} \frac{x - X_y}{\sqrt{y_0}}} \right) \right] e^{-\gamma_0(x - X_y)}. \quad (66)$$

Finally, we expand in power series of λ , using the identity

$$(1-\lambda) \ln \frac{1}{1-\lambda} = \lambda - \sum_{k \geq 2} \frac{\lambda^k}{k(k-1)}. \quad (67)$$

⁵This condition limits the values of k we may reach through our calculation to numbers much smaller than $\mathcal{O}(e^{\text{const} \times \sqrt{y_0}})$; but this is parametrically a very large number when $y_0 \gg 1$.

It is then straightforward to check that we get back Eq. (54) for the coefficient w_1 of $(-\lambda)$ in this series (in the same approximations), and Eq. (48) for the coefficient w_k of $(-\lambda^k)$ in the case $k \geq 2$.

Let us comment that the proposed conjecture does not only apply to the present context, but applies also much more generally to a large class of branching random walk models. This allows for accurate checks: indeed, we can pick a model easy to implement numerically and to run, and

solve it for the delay. Such a calculation is reported in the Appendix and shows perfect consistency with our conjecture. The good matching of our numerical calculation with the conjecture brings, in turn, strong support for the expressions of the weights w_k we have found from the phenomenological model, since they are fully determined by the delay of the traveling wave in the present approach.

IV. DIFFRACTIVE CROSS SECTION AND GAP DISTRIBUTION

We are now in a position to come back to the physical observables, and with the help of the results we have obtained in the previous section, provide asymptotic expressions. We shall then discuss the problems posed by a standard perturbative formulation.

A. Analytical asymptotics

As argued above, we get the correct parametric expression for σ_{tot} by identifying it to $2w_1$.

As for the diffractive cross section, we get it by summing $2w_k$ over the even values of k , starting with $k = 2$. Using Eq. (48) for $w_{k \geq 2}$ and Eq. (54) for w_1 , we arrive at a very simple expression:

$$\frac{\sigma_{\text{diff}}(y, x; y_0)}{\sigma_{\text{tot}}(y, x)} = \frac{\ln 2}{\gamma_0} \left(\frac{1}{x - X_y} + \sqrt{\frac{2}{\pi\chi''(\gamma_0)}} \frac{1}{\sqrt{y_0}} \right). \quad (68)$$

To get this result, we just needed to use the trivial identity

$$\sum_{\text{even } k \geq 2} \frac{1}{k(k-1)} = \ln 2. \quad (69)$$

This formula for $\sigma_{\text{diff}}/\sigma_{\text{tot}}$ is expected to be valid asymptotically for large y and large y_0 , and for x , chosen in the scaling region, i.e., such that $(x - X_y)^2 \ll y$.

Let us interpret the two terms in Eq. (68). The fluctuation creating a large dipole, that scatters elastically off the nucleus, happens most likely either in the beginning of the evolution (leading to a dissociative but small mass event) or close to the scattering rapidity \tilde{y}_0 (leading to a gap of size close to y_0). The first configuration is dominant when y_0 is chosen large compared to $(x - X_y)^2$, leading to the first term in Eq. (68). The second configuration is dominant when y_0 is chosen small compared to $(x - X_y)^2$: in this case, the second, y_0 -dependent, term dominates the diffractive cross section.

In the same way, starting from Eqs. (17), (24) and using the analytical expression (44), we find that the rapidity gap distribution in the scaling region reads

$$\pi(y, x; y_{\text{gap}}) = \frac{\ln 2}{\gamma_0 \sqrt{2\pi\chi''(\gamma_0)}} \left(\frac{y}{y_{\text{gap}}(y - y_{\text{gap}})} \right)^{3/2} \times \exp\left(-\frac{(x - X_y)^2}{2\chi''(\gamma_0)(y - y_{\text{gap}})}\right). \quad (70)$$

Equation (68) is an integral of Eq. (70) over y_{gap} , in the limit $x, y \rightarrow +\infty$, keeping $x - X_y$ fixed. The determination of the overall constant is the main new result in this work, while the functional dependence was first found in Ref. [16].

This expression is tantamount to that of the distribution of the splitting rapidity of the most recent common ancestor of the set of dipoles which scatter derived in Ref. [32], up to an extra factor $\ln 2$. This distribution, denoted by $G(y, x; y_1)/T(y, x)$ in the latter paper, can be expressed with the help of our weights w_k as

$$\frac{G(y, x; y_1)}{T(y, x)} = \frac{\sum_{k=2}^{\infty} \partial_{\tilde{y}_1} w_k(y, x; y - \tilde{y}_1)}{\sum_{k=1}^{\infty} w_k(y, x; y_1)}. \quad (71)$$

Inserting the expression (44) for the $\partial_{\tilde{y}_1} w_k$ s into the numerator and replacing the denominator by its leading term w_1 given in Eq. (54), we recover the analytical form found in Ref. [32]. The factor $\ln 2$ present in Eq. (70) does not appear here, basically because the summation (69) to arrive at the gap distribution is replaced by $\sum_{k \geq 2} 1/[k(k-1)]$, which is unity.

B. On the relation to the standard perturbative approach

The formulation of the observables we are considering has involved the probabilistic weights $w_k = \langle G_k \rangle$ of the contribution of k participant dipoles exactly. These quantities are probabilities in the dipole model, but they have no simple diagrammatic interpretation: rather, they resum an infinity of diagrams, involving an arbitrary number of participating dipoles.

The standard approach consists instead in computing forward elastic scattering amplitudes in perturbation theory, order by order in the number of rescatterings. The contribution of each graph to the considered observable is then obtained by applying the Abramovsky-Gribov-Kancheli cutting rules [40]. The latter were initially established in the context of Regge theory, and argued to also hold in QCD [41]. The KL equation was proved to be consistent with these rules [14].

In the formalism we have used in this paper, this approach corresponds to expanding the observables as series of $\langle F_N(I) \rangle$, where the F_N s were defined in Eq. (19). Indeed, one may write

$$\sigma_{\text{tot}}(y, x) = 2 \sum_{N=1}^{\infty} (-1)^{N+1} \langle F_N[I(y_0)] \rangle_{\tilde{y}_0, x},$$

$$\sigma_{\text{in}}(y, x) = \sum_{N=1}^{\infty} (-2)^{N+1} \langle F_N[I(y_0)] \rangle_{\tilde{y}_0, x}, \quad (72)$$

the diffractive cross section following from the difference of the total and the inelastic cross sections. (See also Ref. [42] for a discussion of these formulas starting from the Abramovsky-Gribov-Kancheli rules.) Note that the terms of order N of these series are related to the N th derivative of the generating function \tilde{w}_λ , but evaluated at $\lambda = 1$ instead of $\lambda = 0$ as in the case of the w_k s.

But, as shown in Ref. [43,44], the expansions (72) turn out to be impractical to compute observables such as the total or diffractive cross sections in the scaling region, where unitarity corrections are important: indeed, they were shown to be severely divergent asymptotic series, and a Borel resummation is required to arrive at a meaningful result.

V. CONCLUSION AND OUTLOOK

To summarize, we have found a purely probabilistic formulation of diffractive onium-nucleus scattering, that we expect to hold rigorously for large-enough values of the rapidities. The very existence of such a formulation is already surprising enough, since diffraction is a typical quantum mechanical phenomenon, with no classical counterpart.

This formulation has enabled us to derive a parameter-free expression for the ratio of the diffractive cross section with a fixed minimum rapidity gap to the total cross section, in the geometric scaling region and for large rapidities, as well as for the gap distribution. In variables relevant to the scattering of an onium of size r off a large nucleus at relative rapidity Y , this ratio reads [see Eq. (68)]

$$\frac{\sigma_{\text{diff}}(Y, r; Y_0)}{\sigma_{\text{tot}}(Y, r)} = \frac{\ln 2}{\gamma_0} \left(\frac{1}{2 \ln[1/r Q_s(Y)]} + \sqrt{\frac{2}{\pi \chi''(\gamma_0) \sqrt{\bar{\alpha} Y_0}}} \right), \quad (73)$$

where the Y -dependent saturation scale in units of the McLerran-Venugopalan momentum evolves as $\ln[Q_s^2(Y)/Q_A^2] = \chi'(\gamma_0) \bar{\alpha} Y - 3/(2\gamma_0) \ln(\bar{\alpha} Y)$. The gap distribution reads [see Eq. (70)]

$$\pi(Y, r; Y_{\text{gap}}) = \frac{\ln 2}{\gamma_0 \sqrt{2\pi \chi''(\gamma_0)}} \frac{1}{\sqrt{\bar{\alpha}}} \left(\frac{Y}{Y_{\text{gap}}(Y - Y_{\text{gap}})} \right)^{3/2} \times \exp \left(-\frac{\ln^2[r^2 Q_s^2(Y)]}{2\chi''(\gamma_0) \bar{\alpha} (Y - Y_{\text{gap}})} \right). \quad (74)$$

Along the way, we have found that diffraction is mostly due to the exchange of a large number of color singlets (“Pomerons” in the language of Regge theory) between the onium and the nucleon. Indeed, the distribution w_k of the number k of participant dipoles turns out to go like $1/[k(k-1)]$. (Let us note that an equation for the moments of the dipole multiplicity has been established very recently, see Ref. [45]).

We believe that the present work paves the way for a number of future developments. On the formal side, a more rigorous derivation of the weights w_k for general branching random walks would be of great interest, since the latter processes and their observables are of potential relevance to different fields of science. The generating function method exposed in Sec. III B looks a promising starting point. Also, finding a systematic way to compute the subleading corrections would be extremely useful. Knowing the next-to-leading order corrections, presumably of relative order $\ln \bar{\alpha} Y / \sqrt{\bar{\alpha} Y}$ or $1/\sqrt{\bar{\alpha} Y}$, would already enable us to extend sizably the kinematical range in which the asymptotic formulas are close to an exact calculation.

Diffraction in onium-nucleus scattering can easily be related to the same process in electron-ion collisions. But approaching closely our analytical results would require rapidities that are not reachable at colliders. Nevertheless, since Eqs. (73) and (74) should represent the exact asymptotics of the KL equation, which follow from QCD, they may be regarded as a solid theoretical starting point for the construction of a realistic model for diffractive dissociation in deep-inelastic scattering off a large nucleus and in the kinematics of a future electron-ion collider (see, e.g., [46,47]), built in such a way that it matches, in the appropriate limits, the asymptotics we have found. A recent numerical study of the KL equation [48] has illustrated that the general trend of these asymptotics may be observed experimentally, up to a significant smearing due to sub-asymptotic corrections yet to be understood theoretically.

Finally, let us mention that the KL equation was also studied theoretically, with phenomenological applications to the DESY-HERA data, in Ref. [49]. The thrust was however different. First, the considered process was deep-inelastic scattering off a proton rather than off a large nucleus. Consequently, the impact parameter dependence was a crucial ingredient, while in our calculation targeted at very large nuclei, we could safely neglect it. Second, all kinematical regions were investigated in Ref. [49], from the saturation region in which the S matrix is close to zero to the regime of very weak scattering, while we have strictly focused on the scaling region. In the region in which we overlap, we believe that our results (73), (74) are more complete. The main difference is in the nontrivial rapidity dependence we have found in the ratio of the diffractive to the total cross section (that was actually already argued—but not derived—in Refs. [16,17]), which was not found in Ref. [49]. In a nutshell, the mismatch can be traced back to the subleading power correction to the exponential dependence of the saturation scale upon the rapidity, which was neglected in Ref. [49].

ACKNOWLEDGMENTS

The work of A. D. L. and S. M. is supported in part by the Agence Nationale de la Recherche under Project No. ANR-16-CE31-0019. The work of A. H. M. is

supported in part by the U.S. Department of Energy Grant No. DE-FG02-92ER40699.

APPENDIX: NUMERICAL CHECK OF THE CONJECTURED DELAY FUNCTION

In this Appendix, we check that the conjecture in Eq. (60) is consistent with numerical calculations. Our goal is not to present QCD calculations in the kinematics of actual colliders, but, instead, to check as accurately as possible our theoretical conjecture and calculations. Therefore, we pick a simple branching random walk model, and push y to the largest possible values that allows a calculation of the delay with reasonable computer resources.

As for the specific model, we consider the well-tested discretization of the branching Brownian motion introduced in Ref. [50] and further studied in Ref. [32]. We refer the reader to the latter articles for a complete description of the model, and in particular, for the numerical values of the constants that replace γ_0 and $\chi''(\gamma_0)$ in Eq. (60).

We solve numerically the equivalent BK equation in the form $BK_{\mathfrak{F}}$ (which rules the evolution of $1 - \tilde{w}$): for our model, it is a discretization of the Fisher and Kolmogorov-Petrovsky-Piscounov equation. We start with a sharp step (tantamount to the McLerran-Venugopalan T -matrix element), and evolve it to the rapidity y_0 . Then, either we evolve further to the final rapidity y at which we measure the delay, or we multiply the front by $1 - \lambda$, and evolve this new initial condition for $\tilde{y}_0 \equiv y - y_0$ more time steps. We eventually compute the difference in the position between

the two fronts we obtain: the number we get is the “delay” we aim at studying.

In the case of a continuous model such as QCD, we could get this delay by evaluating the integral

$$\int_{-\infty}^{+\infty} dx [\tilde{w}_0(y, x; y_0) - \tilde{w}_\lambda(y, x; y_0)] \equiv f_{y_0; y}^{\text{num}}(\lambda). \quad (\text{A1})$$

(Note that it has a y dependence since numerical calculations are necessarily performed for finite y .) The integral in the left-hand side is straightforwardly discretized to be taken over to the model we have implemented. We repeat the calculation of the delay for different values of λ , y , and $y_0 < y$.

The results are shown in Fig. 2. The upper set of points represents the numerical data for the delay rescaled by $f_\infty(\lambda)$ and subtracted from 1 (which is the expected infinite- y_0 limit of this rescaled delay). The data is compared to the conjectured function at finite y_0 , which reads $\frac{1}{\gamma_0} \sqrt{\frac{2}{\pi \chi''(\gamma_0)}} \frac{1}{\sqrt{y_0}}$. We pick two different values of the parameter λ , namely $\lambda = 0.01$ and $\lambda = 0.9$, and for each λ , three values of y : 10^4 , 10^5 , 10^6 .

We see that in the relevant parametric domain in which we expect our conjecture to be valid, namely $1 \ll y_0 \ll y$, all data points almost superimpose, and approach closely the graph of the conjectured function. The agreement is better for larger y , due to the extension of the range in y_0 of validity of the approximations.

The lower set of points represents the difference of the data and the conjecture. We see that the mismatch is

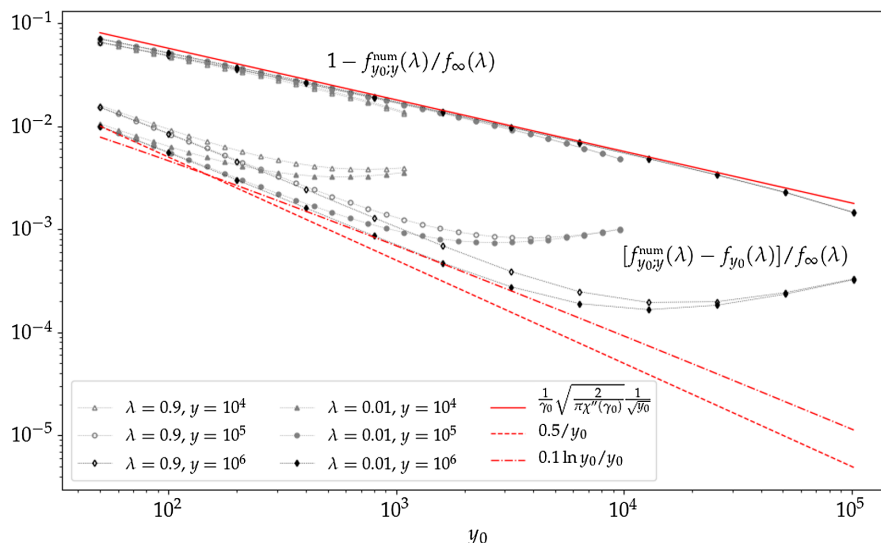


FIG. 2. Comparison of the front delay calculated by solving numerically the exact evolution equation and of the conjectured formula (60), as a function of y_0 . The points represent the data for $1 - f_{y_0}^{\text{num}}(\lambda)/f_\infty(\lambda)$, which should tend to $\frac{1}{\gamma_0} \sqrt{\frac{2}{\pi \chi''(\gamma_0)}} \frac{1}{\sqrt{y_0}}$ at large y , see Eq. (60) (full line), and the distance $[f_{y_0}^{\text{num}}(\lambda) - f_{y_0}(\lambda)]/f_\infty(\lambda)$ between the full model and the conjectured asymptotics. Two different values of λ have been considered (0.9 and 0.01), and for each λ , three different values of y (10^4 , 10^5 , 10^6). The dashed line and dashed-dotted lines are the graphs of functions proportional to $1/y_0$ and $\ln y_0/y_0$, respectively.

consistent with a function that decreases with y_0 as $1/y_0$, or at most as $\ln y_0/y_0$.

Let us mention that we have also checked directly (by solving the equivalent KL equation for this model) that the rapidity-gap distribution itself does indeed converge, for large rapidities, to the predicted form (70). We do not report on these numerical calculations here, because the results look very similar to those for the distribution

$G(y, x; y_1)/T(y, x)$ of the splitting rapidity \tilde{y}_1 of the last common ancestor of all dipoles of log inverse size larger than x : the latter was calculated analytically and numerically in Ref. [32]. The gap distribution and G/T turn out to have the same large-rapidity asymptotics, except for the extra factor $\ln 2$ present in the expression of the former, which we have checked numerically to be correct. The finite-rapidity corrections exhibit the same patterns.

-
- [1] G. Alberi and G. Goggi, Diffraction of subnuclear waves, *Phys. Rep.* **74**, 1 (1981).
- [2] K. A. Goulianos, Diffractive interactions of hadrons at high-energies, *Phys. Rep.* **101**, 169 (1983).
- [3] T. Ahmed *et al.* (H1 Collaboration), First measurement of the deep inelastic structure of proton diffraction, *Phys. Lett. B* **348**, 681 (1995).
- [4] M. Derrick *et al.* (ZEUS Collaboration), Measurement of the diffractive structure function in deep elastic scattering at HERA, *Z. Phys. C* **68**, 569 (1995).
- [5] L. Schoeffel, Advances in diffraction of subnuclear waves, *Prog. Part. Nucl. Phys.* **65**, 9 (2010).
- [6] A. Accardi *et al.*, Electron ion collider: The next QCD frontier: Understanding the glue that binds us all, *Eur. Phys. J. A* **52**, 268 (2016).
- [7] P. Agostini *et al.* (LHeC and FCC-he Study Group), The large hadron-electron collider at the HL-LHC, [arXiv:2007.14491](https://arxiv.org/abs/2007.14491).
- [8] D. Bendova, J. Cepila, J. G. Contreras, V. P. Gonçalves, and M. Matas, Diffractive deeply inelastic scattering in future electron-ion colliders, *Eur. Phys. J. C* **81**, 211 (2021).
- [9] N. N. Nikolaev and B. Zakharov, Color transparency and scaling properties of nuclear shadowing in deep inelastic scattering, *Z. Phys. C* **49**, 607 (1991).
- [10] C. Ewerz and O. Nachtmann, Towards a nonperturbative foundation of the dipole picture. II. High energy limit, *Ann. Phys. (Amsterdam)* **322**, 1670 (2007).
- [11] Y. V. Kovchegov and E. Levin, *Quantum Chromodynamics at High Energy, Cambridge Monographs on Particle Physics, Nuclear Physics and Cosmology* (Cambridge University Press, Cambridge England, 2012), .
- [12] H. Mäntysaari, Review of proton and nuclear shape fluctuations at high energy, *Rep. Prog. Phys.* **83**, 082201 (2020).
- [13] K. J. Golec-Biernat and M. Wusthoff, Saturation effects in deep inelastic scattering at low Q^2 and its implications on diffraction, *Phys. Rev. D* **59**, 014017 (1998).
- [14] Y. V. Kovchegov and E. Levin, Diffractive dissociation including multiple pomeron exchanges in high parton density QCD, *Nucl. Phys.* **B577**, 221 (2000).
- [15] E. Levin and M. Lublinsky, Nonlinear evolution and high-energy diffractive production, *Phys. Lett. B* **521**, 233 (2001).
- [16] A. H. Mueller and S. Munier, Diffractive Electron-Nucleus Scattering and Ancestry in Branching Random Walks, *Phys. Rev. Lett.* **121**, 082001 (2018).
- [17] A. H. Mueller and S. Munier, Rapidity gap distribution in diffractive deep-inelastic scattering and parton genealogy, *Phys. Rev. D* **98**, 034021 (2018).
- [18] A. M. Stasto, K. J. Golec-Biernat, and J. Kwiecinski, Geometric Scaling for the Total Γ^*p Cross-Section in the Low x Region, *Phys. Rev. Lett.* **86**, 596 (2001).
- [19] C. Contreras, E. Levin, R. Meneses, and I. Potashnikova, DGLAP evolution for DIS diffraction production of high masses, *Eur. Phys. J. C* **78**, 699 (2018).
- [20] I. Balitsky, Operator expansion for high-energy scattering, *Nucl. Phys.* **B463**, 99 (1996).
- [21] Y. V. Kovchegov, Unitarization of the BFKL pomeron on a nucleus, *Phys. Rev. D* **61**, 074018 (2000).
- [22] A. H. Mueller, Soft gluons in the infinite momentum wave function and the BFKL pomeron, *Nucl. Phys.* **B415**, 373 (1994).
- [23] S. Munier, Quantum chromodynamics at high energy and statistical physics, *Phys. Rep.* **473**, 1 (2009).
- [24] L. D. McLerran and R. Venugopalan, Computing quark and gluon distribution functions for very large nuclei, *Phys. Rev. D* **49**, 2233 (1994).
- [25] S. Munier and R. B. Peschanski, Geometric Scaling as Traveling Waves, *Phys. Rev. Lett.* **91**, 232001 (2003).
- [26] L. V. Gribov, E. M. Levin, and M. G. Ryskin, Semihard processes in QCD, *Phys. Rep.* **100**, 1 (1983).
- [27] A. H. Mueller and D. N. Triantafyllopoulos, The energy dependence of the saturation momentum, *Nucl. Phys.* **B640**, 331 (2002).
- [28] W. van Saarloos, Front propagation into unstable states, *Phys. Rep.* **386**, 29 (2003).
- [29] R. A. Fisher, The wave of advance of advantageous genes, *Ann. Eugenics* **7**, 355 (1937).
- [30] A. Kolmogorov, I. Petrovsky, and N. Piscounov, Étude de l'équation de la diffusion avec croissance de la quantité de matière et son application à un problème biologique, *Bull. Univ. État Moscou, A* **1**, 1 (1937).
- [31] A. H. Mueller and S. Munier, Phenomenological picture of fluctuations in branching random walks, *Phys. Rev. E* **90**, 042143 (2014).
- [32] A. D. Le, A. H. Mueller, and S. Munier, Nuclear scattering configurations of onia in different frames, *Phys. Rev. D* **103**, 054031 (2021).
- [33] L. N. Lipatov, Reggeization of the vector meson and the vacuum singularity in nonabelian gauge theories, *Yad. Fiz.* **23**, 642 (1976) [*Sov. J. Nucl. Phys.* **23**, 338 (1976)].

- [34] E. A. Kuraev, L. N. Lipatov, and V. S. Fadin, The Pomeron singularity in nonabelian gauge theories, *Zh. Eksp. Teor. Fiz.* **72**, 377 (1977) [*Sov. Phys. JETP* **45**, 199 (1977)].
- [35] I. I. Balitsky and L. N. Lipatov, The Pomeron singularity in quantum chromodynamics, *Yad. Fiz.* **28**, 1597 (1978) [*Sov. J. Nucl. Phys.* **28**, 822 (1978)].
- [36] E. Brunet and B. Derrida, Shift in the velocity of a front due to a cutoff, *Phys. Rev. E* **56**, 2597 (1997).
- [37] A. H. Mueller and A. I. Shoshi, Small x physics beyond the Kovchegov equation, *Nucl. Phys.* **B692**, 175 (2004).
- [38] É. Brunet and B. Derrida, Statistics at the tip of a branching random walk and the delay of traveling waves, *Europhys. Lett.* **87**, 60010 (2009).
- [39] A. H. Mueller and S. Munier, Particle-number distribution in large fluctuations at the tip of branching random walks, *Phys. Rev. E* **102**, 022104 (2020).
- [40] V. A. Abramovsky, V. N. Gribov, and O. V. Kancheli, Character of inclusive spectra and fluctuations produced in inelastic processes by multi-Pomeron exchange, *Yad. Fiz.* **18**, 595 (1973).
- [41] J. Bartels and M. G. Ryskin, The space-time picture of the Wee partons and the AGK cutting rules in perturbative QCD, *Z. Phys. C* **76**, 241 (1997).
- [42] A. H. Mueller and G. P. Salam, Large multiplicity fluctuations and saturation effects in onium collisions, *Nucl. Phys.* **B475**, 293 (1996).
- [43] A. H. Mueller, Unitarity and the BFKL pomeron, *Nucl. Phys.* **B437**, 107 (1995).
- [44] G. P. Salam, Studies of unitarity at small x using the dipole formulation, *Nucl. Phys.* **B461**, 512 (1996).
- [45] E. Levin, Multiplicity distribution of dipoles in QCD from Le, Mueller and Munier equation, [arXiv:2106.06967](https://arxiv.org/abs/2106.06967).
- [46] N. Armesto, P. R. Newman, W. Słomiński, and A. M. Staśto, Inclusive diffraction in future electron-proton and electron-ion colliders, *Phys. Rev. D* **100**, 074022 (2019).
- [47] J. L. Abelleira Fernandez *et al.*, A large hadron electron collider at CERN Report on the physics and design concepts for machine and detector, *J. Phys. G* **39**, 075001 (2012).
- [48] A. D. Le, Rapidity gap distribution in diffractive dissociation: Predictions for future electron-ion colliders, *Phys. Rev. D* **104**, 014014 (2021).
- [49] C. Contreras, E. Levin, R. Meneses, and I. Potashnikova, CGC/saturation approach: An impact-parameter dependent model for diffraction production in DIS, *Eur. Phys. J. C* **78**, 475 (2018).
- [50] É. Brunet, A. D. Le, A. H. Mueller, and S. Munier, How to generate the tip of branching random walks evolved to large times, *Europhys. Lett.* **131**, 40002 (2020).